12

Subducted and Exhumed Crust beneath Taiwan Imaged by Magnetotelluric Data

Chow-Son Chen[1], Martyn J. Unsworth[2], Chih-Wen Chiang[1,5], Edward Bertrand[3] and Francis. T. Wu[4]

[1]*Institute of Geophysics, National Central University,*
[2]*University of Alberta, Department of Physics, Edmonton,*
[3]*GNS Science, Lower Hutt,*
[4]*Department of Geological Science, State University of New York at Binghamton,*
[5]*Department of Geosciences, National Taiwan University*
[1,5]*Taiwan*
[2]*Canada*
[3]*New Zealand*
[4]*US.*

1. Introduction

Arc-continent collision is widely regarded as a fundamental mode by which continents grow, and the Taiwan orogen has long been considered as a type example of it. In Taiwan, the Luzon Volcanic Arc is actively colliding with the southeast continental margin of China. The Taiwan Orogen is one of the world's most active, with high rates of deformation and seismicity. In addition, due to the oblique nature of convergence between the arc and continental margin, Taiwan offers a unique opportunity to investigate the evolution of arc-continent collision in both time and space (Suppe, 1981). This is possible because variations along strike can be viewed as snapshots of various stages in orogen evolution over time.

In this paper, the general tectonics and geology of Taiwan are briefly reviewed. 2-D inversion models of electrical resistivity using the TAIGER (TAiwan Integrated GEodynamic Research) MT data are then presented. TAIGER is an international geological and geophysical research program initiated in 2004 to study the orogenic processes of Taiwan. Finally, the MT inversion models are interpreted with an intent to answer key questions as to how continents grow and mountains evolve. Specifically:

1. Is orogenic deformation "thin-skinned" or is basement deformation pervasive throughout the system?
2. How does crustal deformation, as expressed in the surface geology, extend into the mantle?
3. How is deformation partitioned laterally as well as vertically in the lithosphere?

2. General background

The Taiwan orogen has developed in response to the collision between the Luzon Volcanic Arc on the Philippine Sea Plate and the continental margin of the Eurasian Plate (Figure 1),

beginning about 3 Ma (Tsai et al., 1977; Teng, 1990). Northeast of Taiwan, the Philippine Sea plate subducts northwestwards beneath the Ryukyu Trench, while south of Taiwan the Eurasian plate is subducting beneath the Philippine Sea plate along the Manila Trench. The convergent boundary (i.e. the suture zone) is marked on land in Taiwan by the Longitudinal Valley (Figure 2; Ho, 1988). The rapid (relative plate convergence is 80 mm/yr; Yu et al., 1997) arc-continental collision is responsible for the dominant geological variations that occur east-west across the island, with rocks generally becoming older and more metamorphosed to the east. The main geological structures are parallel to the strike of the suture in an overall NNE–SSW direction (Figure 2). East of the suture, the Coastal Range (CR) is comprised of accreted Luzon volcanic arc materials that originated on the Philippine Sea plate. West of the suture, the principal geological units are: (1) the Eastern Central Range (ECR or the Tananao schist) that exposes rocks of greenschist facies, (2) the Western Central Range that is comprised of the Backbone (BR) and Hseuhshan Ranges (HSR) and also often referred to as the Taiwan slate belt, (3) the Western Foothills fold-and-thrust belt (WF) and (4) the relatively undeformed Coastal Plains (CP).

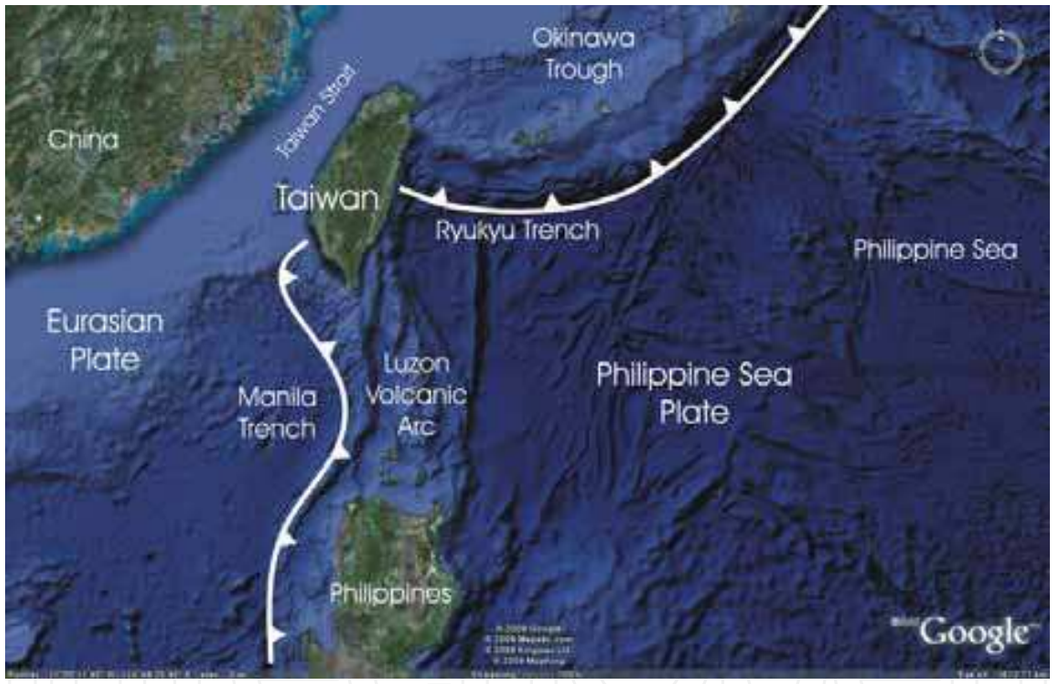

Fig. 1. Regional map of Taiwan showing major geographical and tectonic features. The Eurasian and Philippine Sea Plates are separated by the Ryukyu and Manila Trenches. This map was generated using Google Earth 4.0.2737 software, freely available at http://earth.google.com/

3. Magnetotelluric data collected in Taiwan

MT data were collected on three profiles, NN', CC' and SS' in Taiwan during 2006-2007 (Figure 2). Five-component (three magnetic and two electric) long-period (1-10000s) MT data were recorded at sites spaced ~5 km apart using NIMS instruments designed by Narod Geophysics Ltd. in Canada. To reduce the effects of cultural noise, these long-period MT data were remotely referenced (Gamble et al. 1979) using a station located on the Penghu

archipelago, ~60km from the west coast of the main island of Taiwan. Figure 3 shows one hour of typical time series data recorded simultaneously at a location in central Taiwan (TGR235) and on Penghu (TGR000). Note the similarity of the orthogonal horizontal magnetic fields recorded at these stations, even though they are separated by over 100 km. This similarity occurs because the magnetic fields originate within the ionosphere, far from the Earth's surface. In contrast, the electric and vertical magnetic fields show much greater variation, since they reflect differences in the subsurface electrical resistivity structure (Bertrand, 2010).

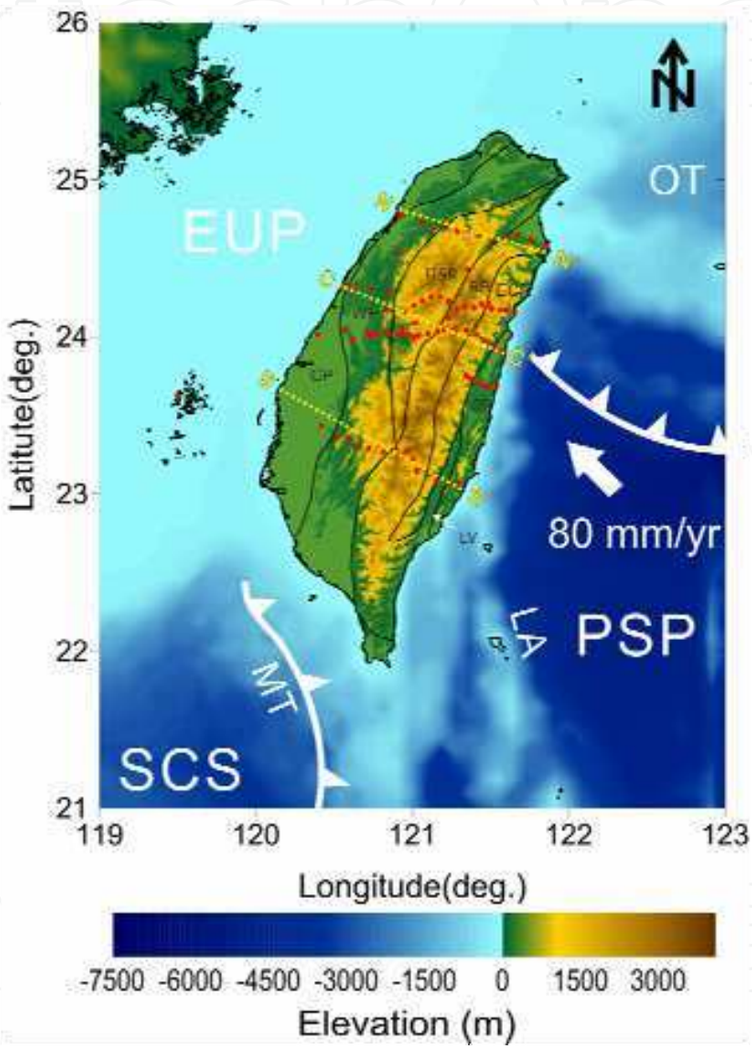

Fig. 2. MT soundings (red) and profiles (yellow) superimposed on the tectonic map of Taiwan. Bold white lines indicate the major convergent boundary between the Philippine Sea and Eurasian Plates. The relative plate motion vector (80 mm/y) of the Philippine Sea Plate with respect to the Eurasian Plate is shown as an arrow. The geological provinces of Taiwan are: CP: Coastal Plain; WF: Western Foothills; HSR: Hsuehshan Range; BR: Backbone Range; ECR: Eastern Central Range; CR: Coastal Range; LV: Longitudinal Valley; EUP: Eurasian Plate; LA: Luzon Volcanic Arc; MT: Manila Trench; OT: Okinawa Trough; PSP: Philippine Sea Plate; SCS: South China Sea. Note that the remote reference MT site on a remote islet west of Taiwan (Figure taken from Chiang, 2010)

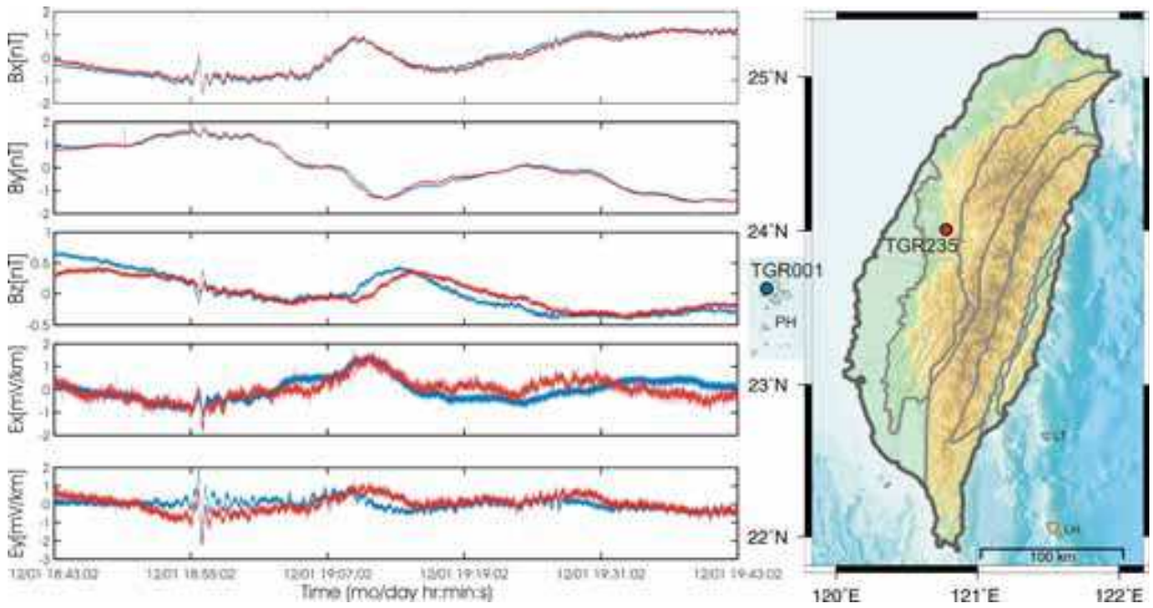

Fig. 3. Simultaneous time series data (60 min) of magnetic and electric fields at station TGR235 (red) in the Western Foothills and at the remote reference station TGR000 on the PH (blue) (Figure taken from Bertrand, 2010)

3.1 Dimensionality analysis

3.1.1 Tensor decomposition – strike angles

Dimensionality analysis from tensor decomposition has been performed on these data using the McNeice-Jones algorithm (McNeice and Jones, 2001). Figure 4 shows the results of the tensor decomposition algorithm (McNeice and Jones, 2001) applied to each MT station individually, and also averaged over the period bands indicated (Bertrand, 2010). Note that strike directions derived from tensor decomposition have an inherent ambiguity of 90°. This 90° ambiguity can be resolved by using external information, such as the regional geological trend. Thus, the geoelectric strike azimuth that closely parallels the average island-strike has been chosen for display. It is clear from the consistent orientation of the bar azimuths that an overwhelming orogen-parallel geoelectric strike direction is determined for these MT data. Furthermore, despite some divergence, at the majority of sites the geoelectric strike remains consistent over all period bands shown. This consistency is an important indication that the MT data on these profiles can be considered 2-D. Closer observation of the strike directions reveals that the dominant azimuth for each profile subtly rotates clockwise from south to north Taiwan. This rotation matches the overall S-shape curvature of the island (Yu et al., 1997) and indicates that the geoelectric strike is consistent with the large-scale 2-D orogen structure and ocean bathymetry (Bertrand, 2010).

3.1.2 Rose diagrams

While the previous map-view plots illustrate the dimensionality of individual MT stations, rose diagrams are advantageous for revealing average data trends (Bertrand, 2010). In Figure 5, rose diagrams are shown that consolidate the results displayed in Figures 4, for data collected on linear profiles. For the main profiles that traverse Taiwan (Lines NN', CC' and SS') the rose diagrams of strike effectively reveal that a dominant 2-D geoelectric strike

direction exists collinear to the island long-axis and major geologic features in Taiwan. The results of this analysis indicate that the electrical structures are two-dimensional with dominant strike directions N45°E, N37°E and N30°E in northern, central and southern Taiwan, respectively (Figure 5). As expected, these strike directions are essentially parallel to the regional geology. The dimensionality analysis presented implies that the generation of 2-D inversion models will be appropriate for these MT data.

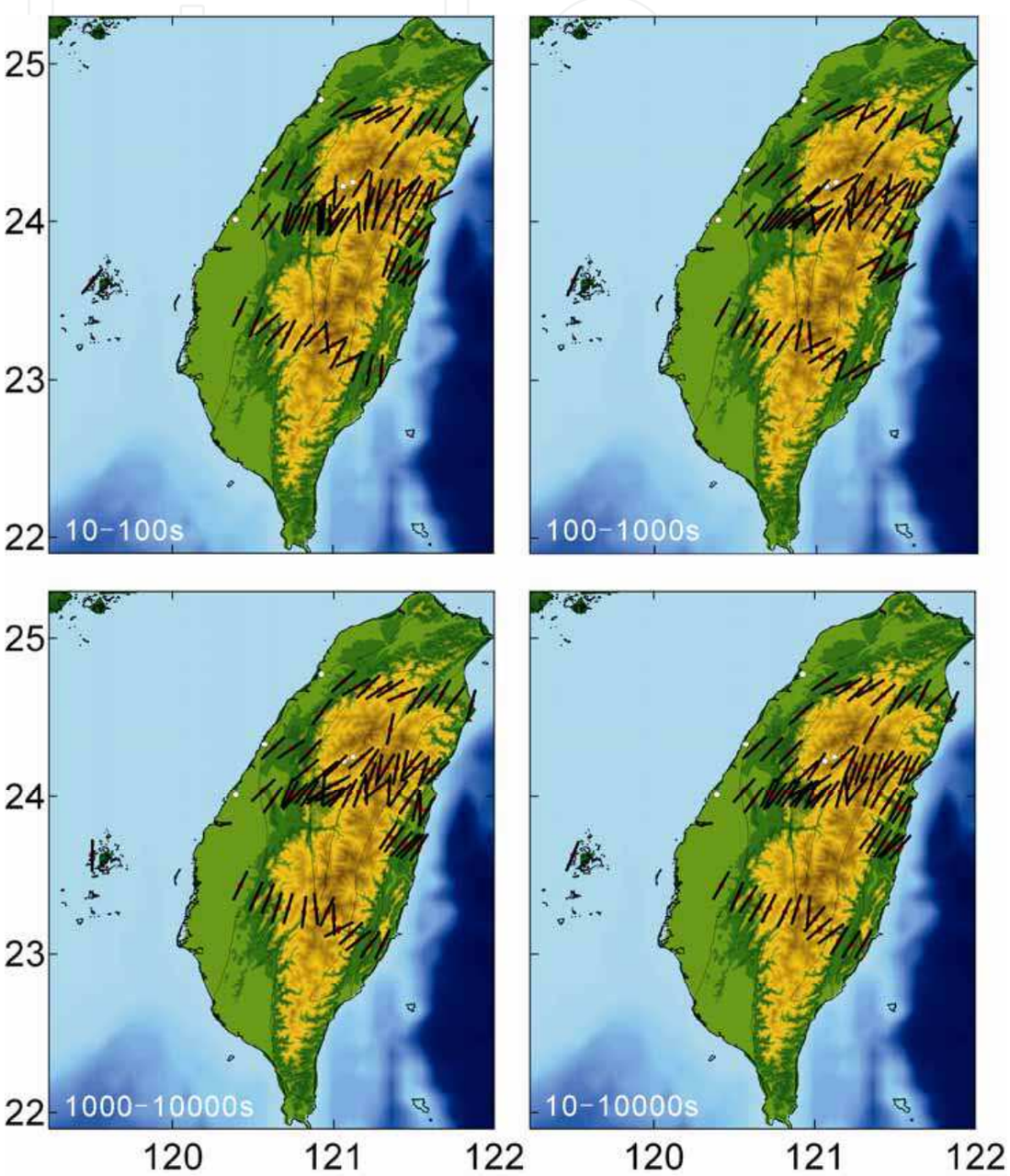

Fig. 4. Geoelectric strike directions determined from single site tensor decomposition for the period range from 10-100s, 100-1000s, 1000-10000s, and 10-10000s (Figure taken from Chiang, 2010)

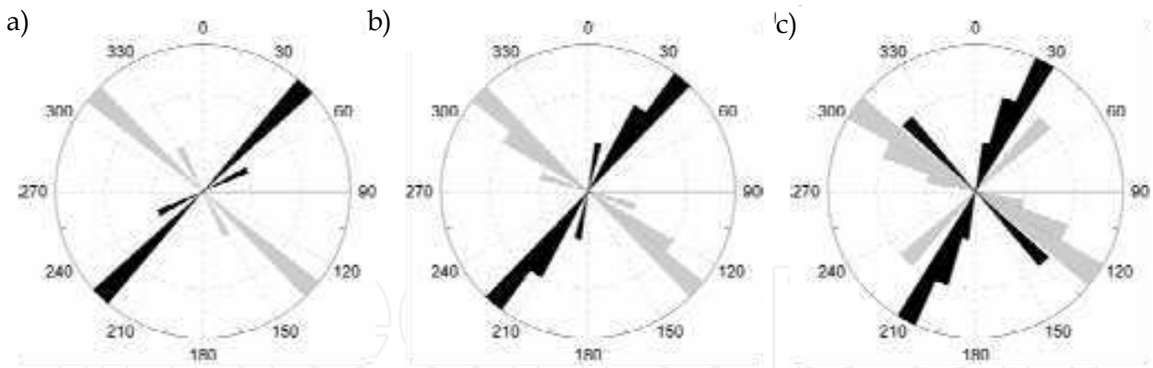

Fig. 5. The rose diagrams show geoelectric strike directions derived from the MT data using tensor decomposition; the electrical structures are two-dimensional with dominant strike directions N45° E (a), N37° E (b) and N30° E (c) in profiles NN', CC' and SS', respectively (Figure taken from Chiang, 2010)

In a 2-D situation, MT data can be separated into two independent modes. The transverse magnetic (TM) mode describes electric currents that flow perpendicular to the geoelectric strike, while electric currents flow parallel to the geoelectric strike in the transverse electric (TE) mode. For each of these modes, the observed MT data along the north, central and south profiles are shown as pseudosections in Figure 6. Note that the differences clearly visible between the TE and TM mode pseudosections indicate that these data are multidimensional, since a 1-D earth would produce MT responses that are identical at all periods and azimuths.

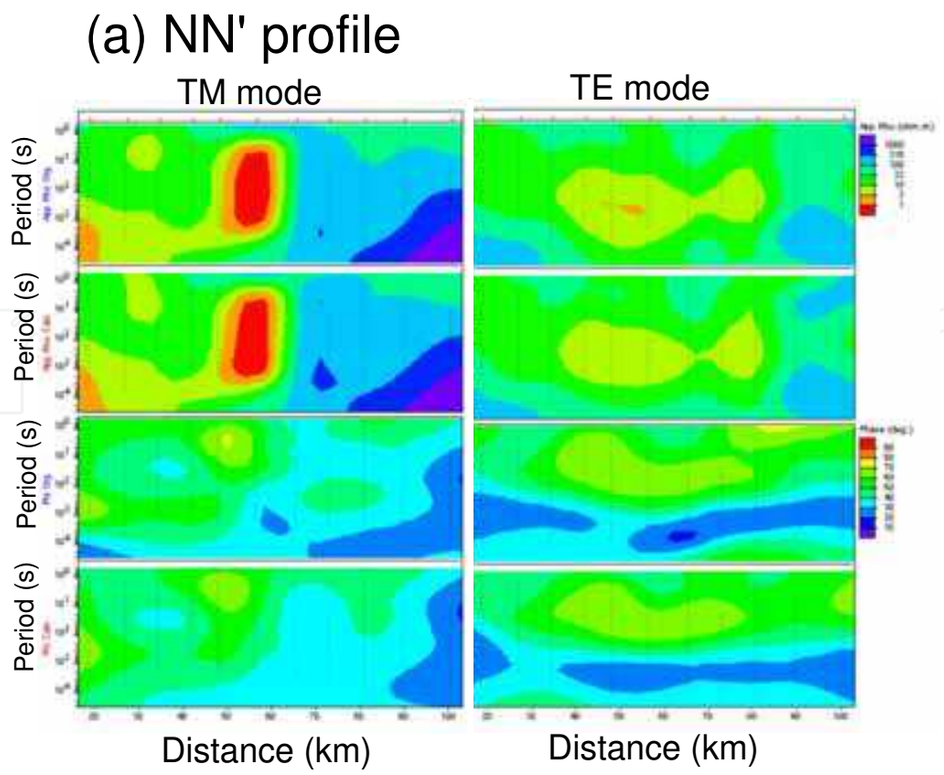

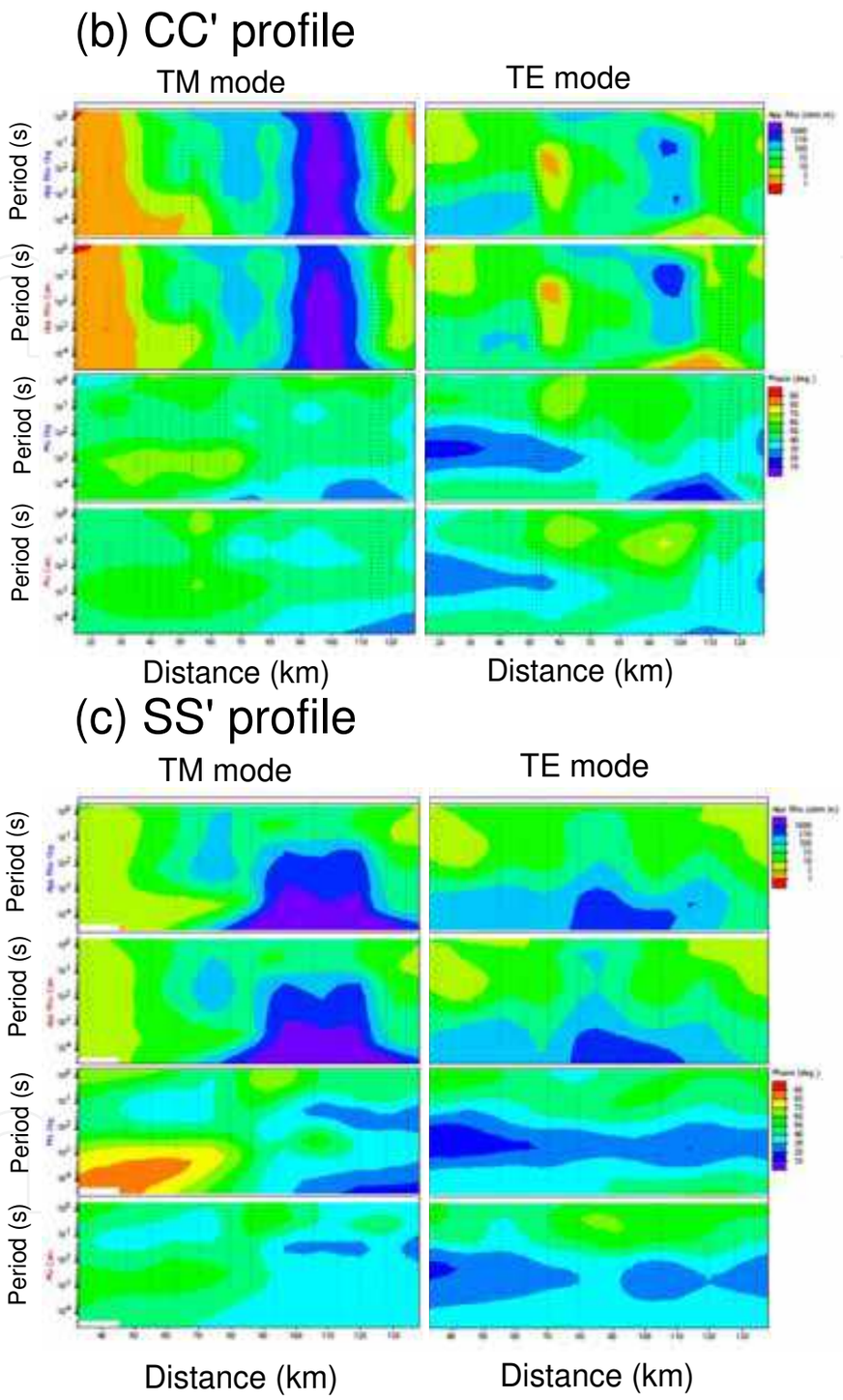

Fig. 6. A comparison between the observed and the calculated pseudo-sections of the joint TE and TM inversion of the three profiles, (a) NN' profile, (b) CC' profile and (c) SS' profile. Dots in each profile are data points. The overall fit between the observed and calculated apparent resistivity and phase of both modes are good, the root-mean-square misfit less than 3.0 for three profiles

3.2 Static shifts

Static shifts in MT data can be caused by electric fields generated from boundary charges on surficial inhomogeneties (Vozoff, 1991). If these inhomogeneities are smaller in size than the skin depth of the highest frequency data recorded, a static (or frequency independent) response can occur that shifts the apparent resistivity estimates up or down by a constant amount (Torres-Verdin and Bostick, 1992). These static shifts are due to under-sampling in both the frequency and spatial domains (Vozoff, 1991). However, instrument and logistical constraints limit the ability to collect closely spaced broadband MT data, especially in mountainous regions.

Therefore, to account for the effects of static shifts in these MT data, large-scale shifts were first removed manually by a detailed comparison of adjacent sites along the profiles. Large-scale shifts can be identified at adjacent sites that show similar apparent resistivity and phase curves, but differ in only the amplitude of the apparent resistivity. Secondly, the 2-D regularized inversion algorithm was set to solve for the remaining small-scale static shifts. Note that by allowing the static shifts to be free parameters, the inversion algorithm solves simultaneously for the apparent resistivity amplitudes and the static shifts. This approach ensures that model structures are not simply due to the incorrect removal of static shifts (deGroot-Hedlin, 1991).

4. Inversion of the MT data

The widely used 2-D magnetotelluric inversion algorithm of Rodi and Mackie (2001) was used to invert the apparent resistivity and phase data on the three profiles traversing north, central and south Taiwan. All inversion models started from a 100 ohm-m half-space that included topography and the ocean bathymetry, and solved for static shifts as described in section 3.2. Error floors of 5% for the phase and 10% for the apparent resistivity were set so that small data errors were increased to these error floor minimums. Inversion models were generated that fit the TE and TM mode data using more than 100 iteration steps and are presented in Figure 7. These inversion models fit the measured MT data to r.m.s. misfit levels of 2.3, 2.8 and 2.9 for NN', CC' and SS', respectively. Comparisons between the observed and the calculated pseudo-sections for these inversion models are shown in Figure 6, and reveal the quality of fit achieved. Note that prior to inversion, these MT data were rotated parallel to the optimum profile geoelectric strike directions of N45°E, N37°E and N30°E, for NN', CC' and SS', respectively. Meanwhile, the smoothing parameters: τ(regularization parameter) = 3 and a(ratio of horizontal to vertical smoothing) = 3 were used for a spatially smooth resistivity model that also produces an acceptable r.m.s. data misfit.

Despite differences between the profile inversion models in Figure 7, each model shows two resistive anomalies R1 (beneath the Western Foothills) and R2 (beneath the Central Ranges). The existence of resistive middle crust is a robust first-order feature of these inversion models.

5. Results

2-D inversion models of the electrical resistivity structure beneath north, central and south Taiwan are displayed in Figure 7; the profile locations are shown in Figure 2. The long-period MT data recorded (station locations are shown at the surface of the inversion models) resolved the electrical structure to depths of ~30 km beneath Taiwan. Seismicity occurring within 15 km of each profile, and of magnitude greater than 4 recorded between 1990 to 2000 by the Central Weather Bureau Seismic Network is also shown on these models. In an

effort to trace crustal components (ie. upper, lower, continental, oceanic) from the developing (southern Taiwan) through to the mature orogen (northern Taiwan), these inversion models are discussed in order from southern to northern Taiwan below.

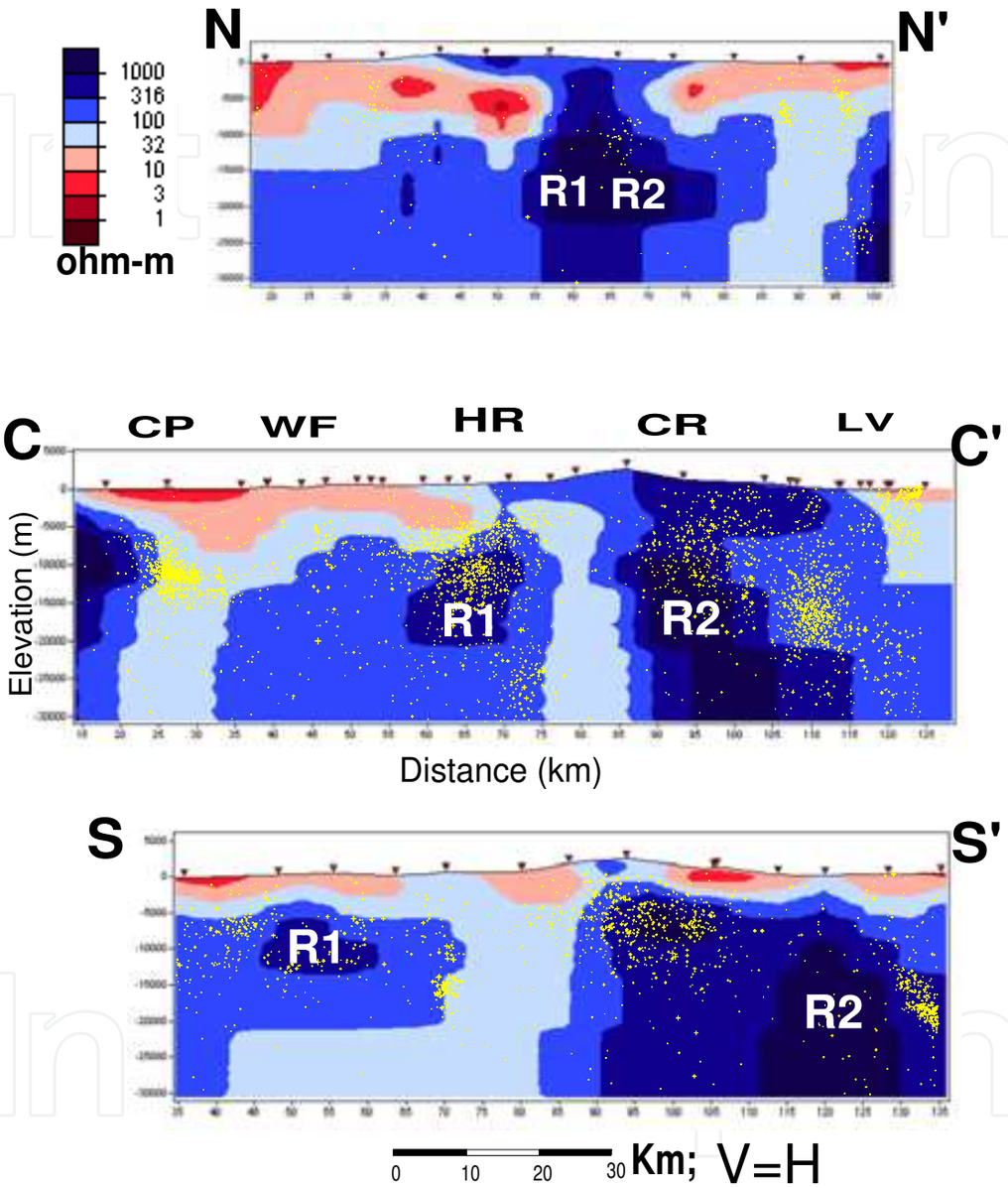

Fig. 7. Subsurface resistivity structures obtained from 2-D inversion of the joint TE and TM inversion of the three profiles, NN', CC' and SS', in Taiwan; the existence of two main resistive anomalies, R1 and R2 locate in the mid-crust beneath the Coastal Plains and Central Range, respectively, account for the response of Taiwan tectonics. The inverted triangles (red) on the surface topography indicate the MT sounding points while the dots (yellow) on the subsurface with magnitudes greater than 4.0 recorded by the Central Weather Bureau Seismic Network (CWBSN) from 1990 to 2000. CP:Coastal Plain; WF:Western Foothills; HR:Hsuehshan Range; CR:Central Range; LV:Longitudinal Valley

5.1 Southern Taiwan profile (S-S')

As previously stated, two high resistivity (>300 ohm-m) zones are imaged in the SS' inversion model. The western region of high resistivity (R1, ~300 ohm-m) is located under the WF, while the eastern zone (R2, 300-1000 ohm-m) occurs beneath the eastern CR. Meanwhile, a thick (~5 km) low resistivity layer is overlain on top of R1. As to the R2, it is found in the mid-crust underneath the eastern higher elevations of the Central Range, where high-grade metamorphic rocks crop out.

Earthquakes in this section occur diffusely and in general scatter around the R1 and R2 high resistivity zones. This spatial relationship is consistent with model of Ague et al., (1998) who suggested that intraplate earthquake swarms are triggered by fluids which migrate into less permeable crust, the less permeable crust may correlate to the high resistivity anomaly regions.

5.2 Central Taiwan profile (C-C')

Although the CC' profile is located ~100 km to the north of the SS' profile, comparison of the MT inversion models shows a similar resistivity structure at each location. In particular, the high resistivity anomalies (R1 and R2) observed in SS' also occur in CC'. However, the distance between R1 and R2 (~30 km) in the central profile is noticeably less than in comparison to the S-S' model (~70 km). Moreover, in comparison to southern Taiwan, R1 is located further east and deeper in central Taiwan, and R2 is shallower and exposed at the surface in the eastern Central Range.

5.3 Northern Taiwan profile (N-N')

Located beneath the mature orogen in Northern Taiwan, where the Philippine Sea Plate contacts the Eurasian Plate at depth (Wu et al., 2010), model NN' shows more variation when compared to the models of CC' and SS', as expected. However, the NN' MT inversion model contains a high resistivity anomaly at mid-crustal depths beneath the Central Ranges that may represent a merger of the R1 and R2 features observed in the models to the south. However, more MT data between the existing profiles is required to trace the along-strike continuation of these features and to ultimately confirm this interpretation. Note that as the northern profile is located in the post-collision zone of the Taiwan orogen, less seismicity is observed in comparison to events plotted on models C-C' and S-S'.

6. Discussion

6.1 Sensitivity test of R1 and R2

It is important to verify that the high-resistivity features observed (R1 and R2 in Figure 7) in the MT inversion models are required by the MT data. To test the model sensitivity to these features, for example profile CC', the high resistivity feature R2 is replaced by background resistivity 100 ohm-m, then fixed model resistivity and inverted with the same parameters as described in section 4. The inversion model fits the measured MT data to r.m.s. misfit levels of 3.72, about 33% increase as compared with the r.m.s. 2.79 before the emplacement. This shows that this high resistivity R2 is required by the MT data. If feature R1 is also replaced by background resistivity 100 ohm-m, the r.m.s. misfit levels is 2.81, only 0.72% increasing. Since high resistivity zone is not well resolved in MT, if located below a conductor. However, if feature R1 is replaced by 1000 ohm-m, 10 times the background resistivity, the r.m.s. misfit levels becomes 3.11, about 11% increase. Thus, both features R2

and R1 appear to be required by the MT data, since decreasing resitivity degrades the fit to the data.

6.2 Resistivity of rock

The electrical resistivity of rocks depends on the density of charge carriers and the geometry of current pathways. High pore fluid salinity, high fluid saturation, and partial melting of rock will all give a high quantity of charge carriers. High porosity, and in particular, good interconnection between pores will yield a favourable network of electric current pathways. The bulk apparent resistivity measured by magnetotelluric data is thus influenced by combinations of the above factors. Although the apparent resistivity of the R1 (~300 ohm-m) and R2 (300~1000 ohm-m) regions are within that of typical mid-to-lower continental crust (10-300 ohm-m) and upper continental mantle (10-3000 ohm-m) (Simpson and Bahr, 2005), to interpret the resistivity images, other constrains are needed for a convincing geologic interpretations, such as seismicity, heat flow, dating and GPS observations, and detailed in next section.

6.3 Crustal subduction and exhumation

Previous papers on inversion models of the TAIGER MT data in central (Bertrand et al., 2009) and southern Taiwan (Chiang et al., 2010) have focused interpretation on the significant low resistivity anomalies that also occur in the models shown in Figure 7. In this chapter, the high resistivity regions are highlighted and additional interpretation is made to investigate the lithospheric structure on the orogen scale.

Arc-continent collision in Taiwan has progressed from north to south and at present has developed an orogen that transitions from young, to mature, to post-collision collapse and extension from south to north Taiwan (Suppe, 1981). Thus, the TAIGER MT data collected on profiles across south, central and north Taiwan can provide information on the evolution of tectonic processes in both time and space beneath the Central Ranges of Taiwan.

As the Eurasian lithospheric mantle enters the subduction zone, the overlying continental crust (interpreted to explain the high resistivity R1 feature in the MT inversion models) beneath the forearc basin could have either been deformed or partially subducted (Chemenda et al. 2001; Lin, 2002). If entrained into the subduction zone, since continental crust is ultimately too bouyant to subduct, the R2 resistivity anomaly (Figure 7) could represent an exhumed crustal slice that is now exposed at the surface in the eastern Central Range.

As described in detail for central (Bertrand et al., 2009) and southern Taiwan (Chiang et al., 2010), it is difficult to explain the subsurface MT resistivity models with the thin-skin tectonic model (Suppe, 1981), that restricts collision related deformation to occur above a shallow decollement. Alternatively, a tectonic model of partial continental subduction followed by crustal exhumation provides a more consistent explanation (Figure 8). The high resistivity regions in the 2-D MT inversion models in Figure 7 can be interpreted to explain general features expected of both the subducted crust (R1) and the exhumed crust (R2). An east-dipping R1 probably reveals active subduction of continental crust of the Eurasian plate beneath the major part of Taiwan. In the southern and central profiles, the boundary between the inferred subducted and exhumed crust (high resistivity anomalies) is marked by a nearly vertical low resistivity anomaly labeled MM' in Figure 8. This boundary occurs between the eastern and western Central Ranges.

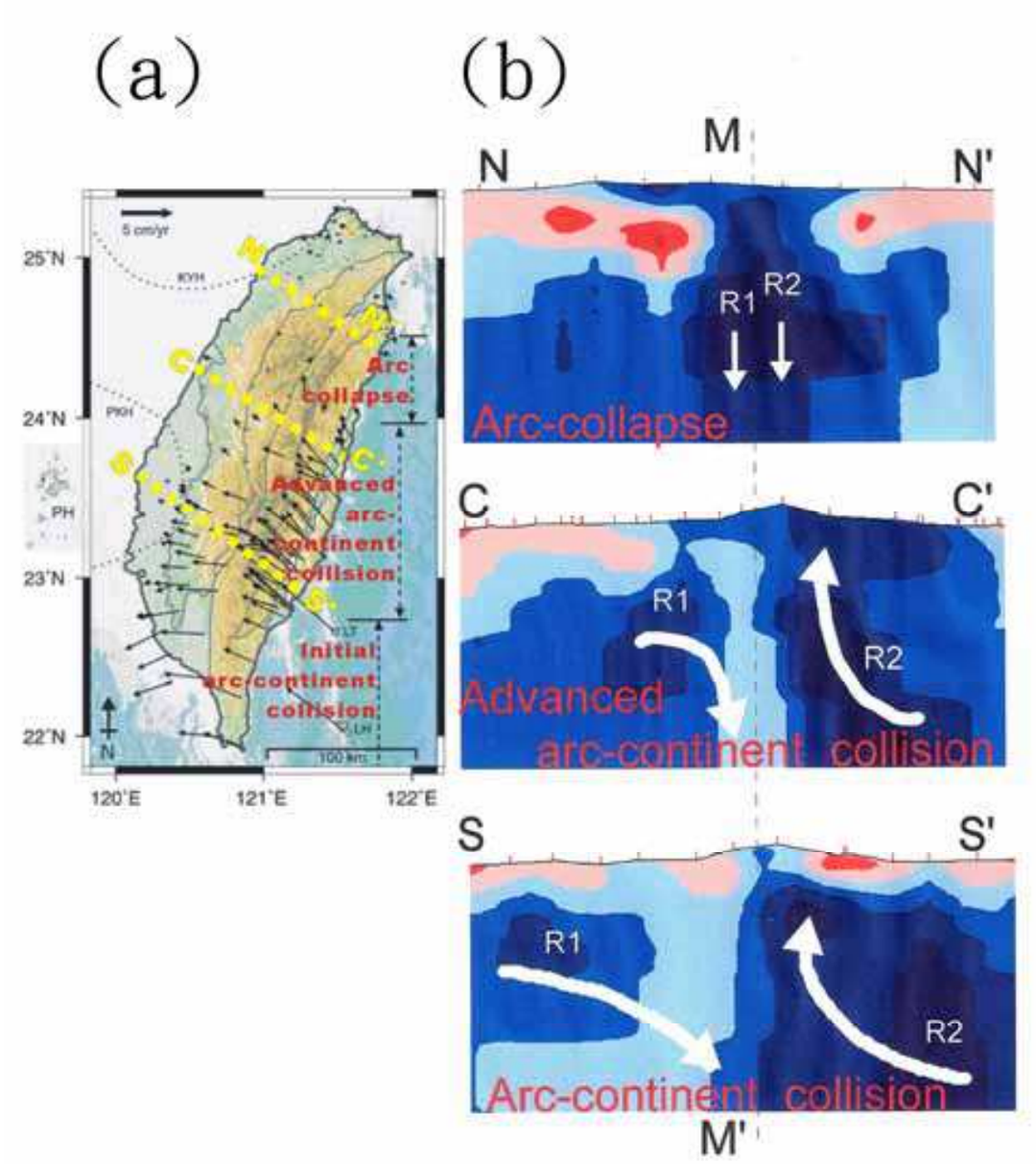

Fig. 8. (a) Locations of MT profiles (yellow hashed lines) and the velocity field of GPS (modified from Bertrand 2010) in Taiwan; the orogeny of Taiwan developed from south to north from developing orogen, mature orogen and post-collision also indicated. (b) Schematic diagrams summarizing the MT results and its interpretations by using the evolution model of active continental subduction, crustal exhumation and then arc collapse. The models are presented in profiles SS', CC' and NN' from south to north. MM' : collision line. Thin dashed lines delineate estimated boundaries of the Peikang (PK) and Kuanyin (KY) basement highs (Mouthereau et al., 2002)

A variety of observations are consistent with the interpretation of R2 as exhumed crust. For example, high heat flow values (~200 mW/m^2; Lin, 2000) and an absence of seismicity (Wu

et al., 1997) have been measured beneath the Central Range. Thus, the high resistivity R2 anomaly imaged in the MT inversion models may represent strong and dry crustal material ascending to shallower depths. Note that the rate of uplift in the central ranges has been suggested to be accelerating during the last million years. Tsao (1996) suggested that the rate of uplift increased from 7 to 16 mm/yr over the past 1.5 Myr, and Liu (1995) conducted leveling measurements that showed rates of uplift of 36–42 mm/y in the eastern Central Range over the past decade.

7. Conclusions

Two mid-crustal, high resistivity regions in the MT inversion models presented above have been interpreted to support a tectonic model of partial crustal subduction and exhumation. With the proposed tectonic model, we can address some key questions as to how continents grow and mountains evolve:

1. Foreland is basement deformation pervasive throughout the orogenic system; the thin-skinned deformation happens at WF at shallow depth.
2. The crustal deformation, as expressed in the surface geology, ultimately root into the mantle, although not displayed in the present resistivity model.
3. The deformation is partitioned, laterally as well as vertically, in the lithosphere.

8. Acknowledgments

The field data were acquired by the joint crew of MT research group of the University of Alberta (Canada) and National Central University (Taiwan). We acknowledge land owners for permissions. Seismicity data were generously supplied by the Central Weather Bureau Seismic Network (CWBSN), Taiwan. This project was funded by the National Science Council of the Republic of China under grants TAIGER: NSC96-2119-M-008-010, NSC97-2745-M-008-015 and NSC98-2116-M-008-011.

9. References

Ague, J., J. Park and D. M.Rye, 1998: Regional metamorphic dehydration and seismic hazard. *Geophys. Res. Lett.*, 25, 4221-4224.

Bertrand, E.A., M.J. Unsworth, C.W. Chiang, C.S. Chen, C. C. Chen, F. Wu, E. Türkoğlu, H.L. Hsu, G. Hill, 2009: Magnetotelluric evidence for thick-skinned tectonics in central Taiwan, *Geology*, 37, 711-714.

Bertrand, E.A., 2010: Magnetotelluric imaging beneath the Taiwan orogen: An arc-continet collision. Ph.D. thesis, University of Alberta, Canada, PP 266.

Chiang, C.W., 2010: Deep electrical structure of Taiwan and its implications. Ph.D. thesis, National Central University, Taiwan, PP 154.

Chiang, C.W., C. C. Chen, M. J. Unsworth, E. A. Bertrand, C. S. Chen, Thong Duy Kieu, and Han-Lun Hsu, 2010. The deep electrical structure of southern Taiwan and its tectonic implications, *Terr. Atmos. Ocean. Sci.*, 21, 879-895.

Chemenda, A.I., R.K. Yang, J.F. Stephan, E.A. Konstantnov skaya, and G.M. Ivanov, 2001: New results from physical modelling of arc-continent collision in Taiwan: evolutionary model. *Tectonophysics*, 333,159–178.

deGroot-Hedlin, C., 1991: Short note: Removal of static shift in two dimensions by regularized inversion, *Geophysics*, 56, 2102-2136.

Gamble, T. D., W. M. Goubau. and J. Clarke, 1979: Magnetotellurics with a remote reference. *Geophysics*, 44, 53–68.

Ho, C.S., 1988: An introduction to the geology of Taiwan, explanatory text of the geologic map of Taiwan: Taipei, Taiwan, 192 p.

Lin, C. H., 2002: Active continental subduction and crustal exhumation: the Taiwan orogeny. *Terra Nova*, 14, 281–287.

Liu, C. H., 1995: Geodetic monitoring of mountain building in Taiwan (abstr.). Eos, Trans. *Am. Geophys. Un.*, 76, 636.

McNeice, G. W. and A. G. Jones, 2001: Multi-site, multi-frequency tensor decomposition of magnetotelluric data, *Geophysics*, 66, 158-173.

Mouthereau, F., B. Deffontaines, O. Lacombe and J. Angelier, 2002: Variations along the strike of the Taiwan thrust belt: Basement control on structural style, wedge geometry and kinematics, in Byrne, T.B. and C.S. Liu, eds., Geology and Geophysics of an Arc-Continent Collision, Taiwan: Boulder, Colorado, *Geological Society of America Special Paper 358*, 31-54.

Rodi, W. and R. L. Mackie, 2001: Nonlinear conjugate gradients algorithm for 2-D magnetotelluric inversion. *Geophysics,* 66, 174– 187.

Simpson, F., and K. Bahr, 2005: Practical Magnetotellurics, Cambridge University Press, 254 pp.

Suppe, J., 1981: Mechanics of mountain building in Taiwan. *Mem. Geol. Soc. China*, 4, 67–89.

Teng, L. S., 1990: Geotectonic evolution of late Cenozoic arc-continental collision in Taiwan. *Tectonophysics*, 183, 57-76.

Torres-Verdin, C. and F.X., Bostick,1992: Principles of spatial surface electric field filtering in magnetotellurics: Electromagnetic array profiling (EMAP), *Geophysics*, 57, 603-622.

Tsai, Y.B., T.L. Ten, J.M. Chiu and H.L. Liu,1977: Tectonics implications of the seismicity in the Taiwan region. *Mem. Geol. Soc. China*, 2,13–41.

Tsao, S.H., 1996: The geological significance of illite crystallinity, zicon fission-track ages, and K-Ar ages of metasedimentary rocks of the Central Range of Taiwan. Unpubl. *doctoral thesis*, *National Taiwan University*, Taipei, Taiwan.

Vozoff, K., 1991: The Magnetotellruic Method, Chapter 8, Electromagnetic method in applied geophysics-Applications part A and part B, edit by Corbett, J.D., published by *Scociety of Exploration Geophysicists*, 641-711.

Wu, Francis T, R. J. Rau and D. Salzberg, 1997: Taiwan orogeny: thin-skinned or lithospheric collision? *Tectonophysics*, 274, 191-220.

Yu, S.B., H.Y. Chen and L.C. Kuo,1997: Velocity field of GPS stations in the Taiwan area. *Tectonophysics*, 274, 41–59.

New Frontiers in Tectonic Research - General Problems, Sedimentary Basins and Island Arcs

Edited by Prof. Evgenii Sharkov

ISBN 978-953-307-595-2
Hard cover, 350 pages
Publisher InTech
Published online 27, July, 2011
Published in print edition July, 2011

This book is devoted to different aspects of tectonic research. Syntheses of recent and earlier works, combined with new results and interpretations, are presented in this book for diverse tectonic settings. Most of the chapters include up-to-date material of detailed geological investigations, often combined with geophysical data, which can help understand more clearly the essence of mechanisms of different tectonic processes. Some chapters are dedicated to general problems of tectonics. Another block of chapters is devoted to sedimentary basins and special attention in this book is given to tectonic processes on active plate margins.

INTECH
open science | open minds

InTech Europe
University Campus STeP Ri
Slavka Krautzeka 83/A
51000 Rijeka, Croatia
Phone: +385 (51) 770 447
Fax: +385 (51) 686 166
www.intechopen.com

InTech China
Unit 405, Office Block, Hotel Equatorial Shanghai
No.65, Yan An Road (West), Shanghai, 200040, China
中国上海市延安西路65号上海国际贵都大饭店办公楼405单元
Phone: +86-21-62489820
Fax: +86-21-62489821

IntechOpen